UNIT 13 DRAG

Structure

13.1 INTRODUCTION

Several engineering problems such as motion of aeroplanes, submarines and torpedoes; design of fans, turbines, tall buildings, factory shades and bridges etc. require study of flow pattern around these bodies to compute the resistance offered by these bodies to flow. Consider a body placed in an infinite fluid flowing at a steady and uniform velocity. As long as the fluid is real, it will exert a force on the body in the direction of the motion which is known as **drag force**. The body will in turn, exert a force on the fluid equal in magnitude but opposite in direction. This is known as the **resistance**. On the other hand, suppose we consider fluid to be stationary and the body in steady and uniform motion, even then drag force will be exerted on the body. Hence it can be concluded that drag or resitance remains the same whether the body is moving and the fluid is at rest or the fluid is moving and the body is at rest.

The force exerted by the fluid on the body need not necessarily be in the direction of motion. It can make a certain angle with the direction of motion. The component of this force in the direction of motion is known as drag, F_D and the component which is perpendicular to the direction of motion is called lift, F_L. It is worthwhile to mention here that lift force is present when fluid flow is at an angle with respect to the axis of the body i.e. body is asymmetrical in nature.

Whenever flow takes place around the body, there is always a condition of no slip at the surface of contact as well as there is a thin layer of fluid adjacent to the boundary and hence fluid is retarded near the boundary. Therefore, there exists a velocity gradient and hence shear force is caused. Therefore, it can be said that because of presence of viscosity, however small it may be, the flow pattern gets modified by the development of the boundary layer. If such a surface curves away from the flow, there is tendency for the flow to move away from the wall and hence separation of flow takes place. This separation drastically alters the flow pattern and hence the pressure distribution. This affects the drag appreciably.

Objectives

In this Unit, we are going to study basically the forces on bodies immersed in a fluid. For example, a tall building exposed to a strong flow of wind, a sphere falling in a column of liquid. Thus after going through this unit you should be able to

* identify flow pattern around these submerged bodies,
* appreciate the total force exerted by the fluid on the body as well as the components of this force in the direction of flow and in the direction perpendicular to the flow,
* identify the basic geometric and flow parameters influencing these forces,

* clearly understand the phenomenon of separation of flow and its effect on drag force on the body, and
* estimate the drag force for different shapes of the body.

13.2 SEPARATION

Consider flow through a two dimensional expanding channel as shown in Figure 13.1. As the fluid flows from left to right, the velocity of flow decreases because the cross-sectional area is increasing. This reduction in velocity results in increase in the pressure and hence positive pressure gradient is set up. Positive pressure gradient is one in which pressure increases in the direction of flow. The velocity profiles of various sections along the curved surface are shown in Figure 13.1. Initially, as long as $\frac{\partial p}{\partial x}$ is either negative or zero, the fluid velocity either increases or remains constant. In the region of positive pressure gradient, because of decelerating effects, the boundary layer thickness is increased further and does not remain small. Because of thickening of boundary layer, the velocity gradient near the wall decreases in the direction of flow. It can even become zero as shown in the Figure. A further retardation of flow can start back-flow. The flow separates from the boundary from some distance downstream of the point where $\frac{\partial p}{\partial x} = 0$. If all the points below which a reverse flow occurs are joined by a smooth curve AB, it represents the separating stream line. However, location of such a stream line is very difficult, because the point where separation starts, depends on roughness, form of the roughness and Reynolds number.

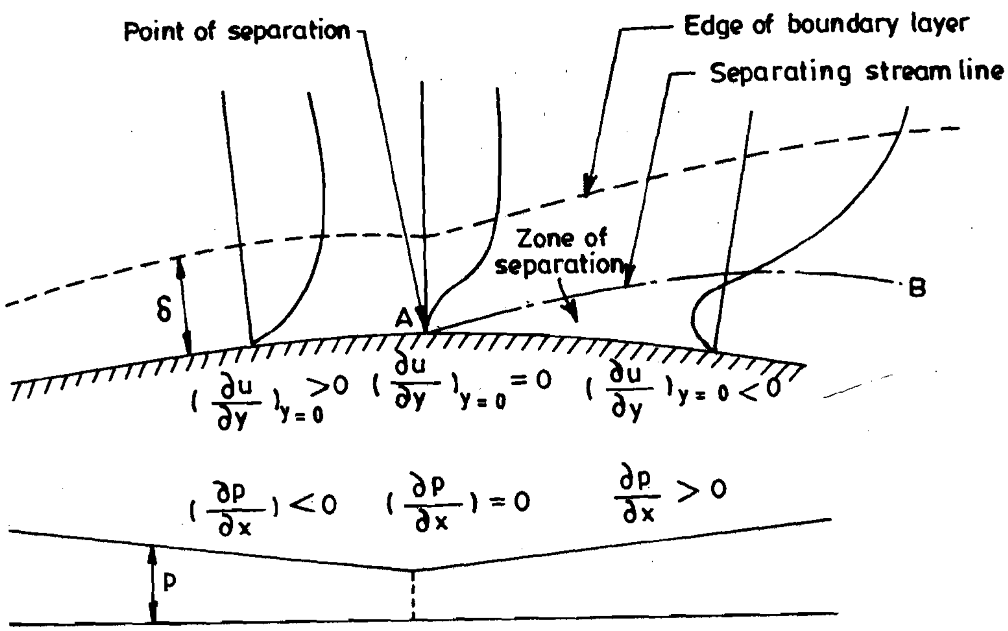

Figure 13.1 : Separation of Boundary Layer in an Expanding Flow

Further, such a stream line oscillates and never remains stationary. Since the separation is affected by retardation of the fluid in the boundary layer, it can been seen that the laminar boundary layer is more susceptible to earlier separation than the turbulent boundary layer.

Due to the reversal of flow, eddies are formed in the region close to the wall. This formation of eddies is accompanied by continuous loss of energy since they derive energy from the main flow for their existence. This energy is ultimately lost as heat. As there is intermittent shedding of these eddies, the body is also subjected to lateral vibrations which are undesirable. Since the separation occurs near the point of minimum pressure and the pressure in the separation zone is essentially constant, such a pressure difference gives rise to longitudinal and some times lateral boundary forces. The net force in the direction of motion caused by this pressure difference is known as **pressure-drag** or **form drag**.

For efficient design of such body shapes, the primary aim is to reduce the tendency for separation and thereby reduce the resistance appreciably. Such problems are encountered in the design of channels and conduit transitions, design of airplanes, ships etc.

13.2.1 Methods of Controlling Separation

The fact that separation originates eddies and these in turn consume energy, calls for control of separation. One way of avoiding separation is to keep the pressure gradient sufficiently small, this is achieved by making the angle of divergence of solid boundaries sufficiently small. This is done by designing diffusers, expanding transitions in open channels with small angle of divergence. The same principle applies to flow past streamlined bodies such as airplane wings.

Separation and backflow takes place when pressure force acts in the opposite direction on fluid particles already slowed down within the boundary layer. Therefore, separation can be delayed if the fluid particles in the boundary layer are accelerated. This can be done by changing laminar boundary layer into turbulent boundary layer by providing artificial roughness. It has been shown in the past that size of the wake behind a sphere can be greatly reduced by providing a thin wire ring as shown in Figure 13.2 (a). This reduces the pressure drag of the sphere appreciably. The same object can be achieved by injecting high velocity fluid in the boundary layer, thereby accelerating the retarded fluid particles as can be seen in Figure 13.2 (c).

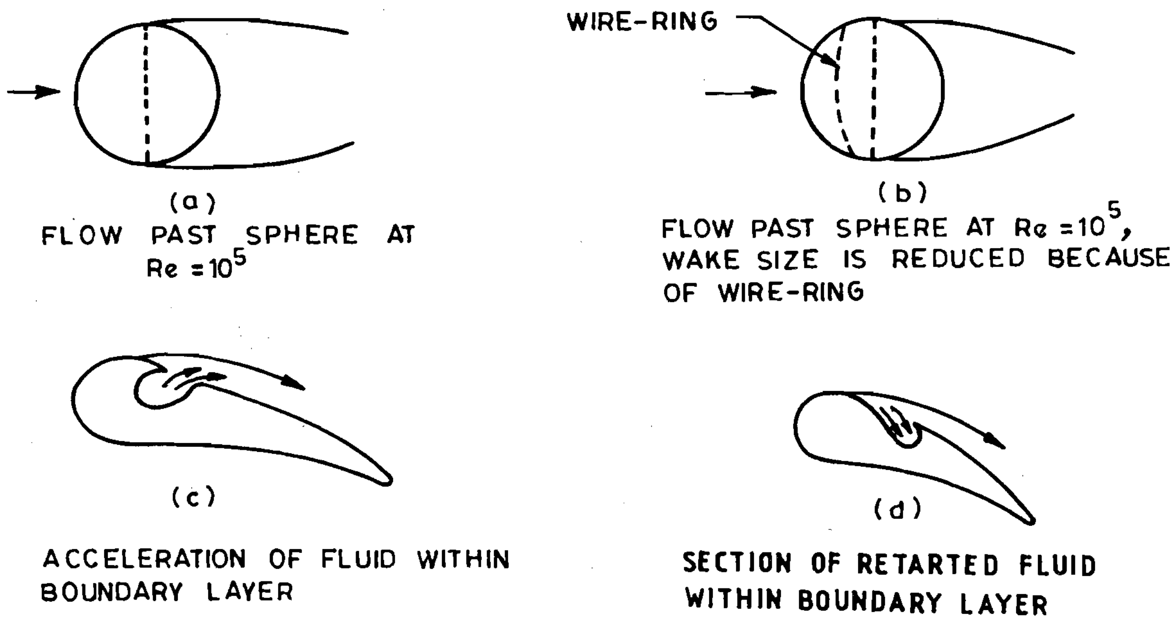

Figure 13.2 : Methods of Boundary Layer Control

The separation can also be controlled by continuously sucking the slow moving fluid from the boundary layer [see Figure 13.2 (d)]. The sucking can be done at one section or along the boundary length. The separation in diverging flows as in bends can be controlled by providing guide vanes as shown in Figure 13.3.

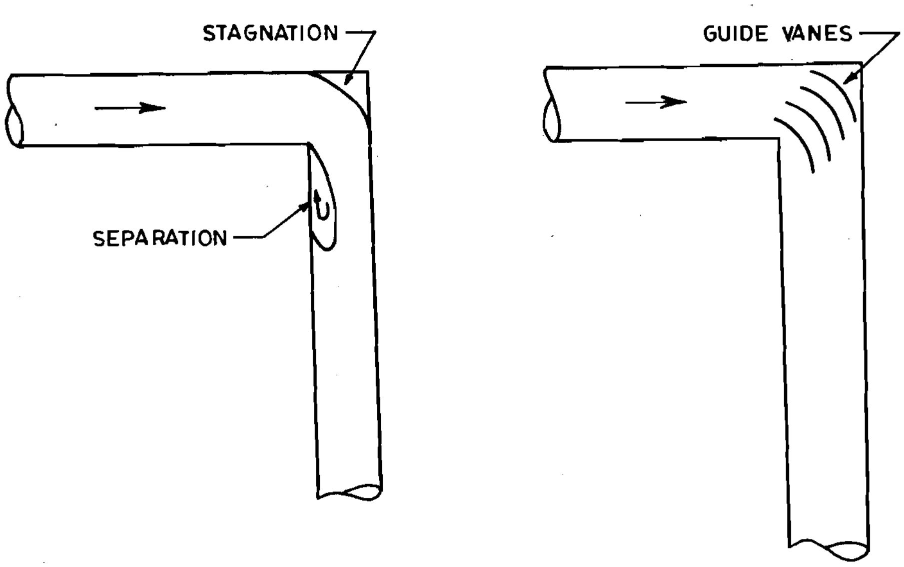

Figure 13.3 : Bends with and without Vanes

SAQ 1

(i) Define drag and lift.

(ii) What is positive pressure gradient?

(iii) Define point of separation.

(iv) List the methods of controlling separation.

13.3 DRAG ON IMMERSED BODIES

Let us consider a body held in a flow of uniform velocity U_0 as shown in Figure 13.4. Let F be the resultant force acting on the body. This total force F can be resolved in two components; the one in the direction of motion known as drag force, F_D and the other perpendicular to the flow known as lift force, F_L. Since the velocities at various points near the surface of the body are different, application of Bernoulli's equation will reveal that pressure at these points also varies. At any point on the surface of the body, two types of forces are acting as shown in the figure. One of them is the shear stress, τ_0, acting in a tangential direction and the other one is pressure force acting perpendicular to the surface. Therefore, this drag force acting in the direction of motion is given by the summation of the components of shear force and pressure force acting over the entire surface of the body.

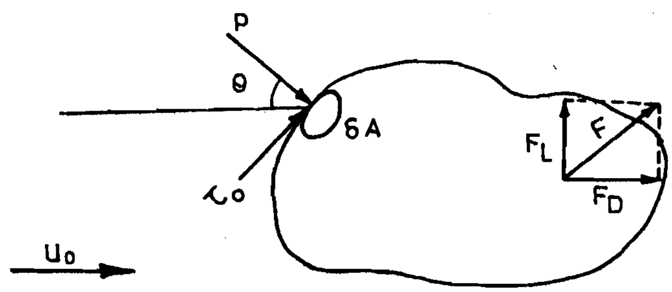

Figure 13.4 : Definition of Drag and Lift

Hence,

$$F_D = \int_A \tau_0 \sin\theta \,\delta A + \int_A p \cos\theta \,\delta A \qquad (13.1)$$

wherein $\int_A$ represents summation over the entire surface area. The relative contribution of each of these to the total drag depends on the shape of the immersed body and on the flow and the fluid characteristics. Thus for the case of flat plate held parallel to the direction of flow, the second term in equation (13.1) will be zero (i.e. $\int_A p \cos\theta \,\delta A = 0$) and hence total drag is only due to viscous shear. On the other hand, if the plate is held perpendicular to the flow, the contribution of the first term will be zero (i.e. $\int_A \tau_0 \sin\theta \,\delta A = 0$) and hence the total drag is only due to variation in pressure. In between these two extremes, there are numereous body shapes for which contribution of the viscous shear to the total drag varies within wide limits depending upon shape of the body and flow conditions.

13.4 DEFORMATION, FRICTION AND FORM DRAGS

The total drag is the sum of deformation drag and form drag. The deformation drag exists at very small velocities i.e. when Reynolds number is very small, preferably less than 0.20. At such small values of Reynolds number, the contribution of inertia force can be neglected as compared to that of viscous force. Under such conditions viscosity influences the flow pattern considerably. In the words of Prandtl and Tietjens, *The body pushes itself through the fluid which is deformed by it. The resistance caused by this is due primarily to the forces necessary for the deformation of various fluid particles*. Smaller the Reynolds number greater is the distance from the body upto which deformation takes place.

The deformation drag consists of friction drag or surface drag at the surface/boundary and the pressure drag due to the variation in pressure caused by wide spread deformation. The proportion of these two for a given body depends very much on the Reynolds number. It has been shown in the past that for the case of a sphere in the Stokes' range, one third of the total drag is due to the pressure difference and two third is due to the surface drag (boundary shear). It has been observed that for the case of disc and sphere of same diameters, if Re is less than 0.1, the total drag of the sphere is slightly higher than that of disc. Considering the fact that the shapes of these two objects are different, the above observation regarding the total drag at low Re reveals that the deformation drag depends very much on the projected area and not much on the shape.

With increase in the Re value, the extent of deformation decreases and is limited to a very thin boundary layer. Because of the reduction in the deformation area, the contribution of the deformation drag almost becomes negligible and the contribution due to the friction drag increases. Thus for higher Re, the direct action of the viscous deformation is the friction drag. At higher values of Re, if the shape of the body is such that separation occurs, low pressure area is created at the rear portion of the body and this produces form drag. Thus the form drag is the result of pressure difference created between front and the rear of the body. The proportions of friction drag and form drag depends very much on the shape of the body and the value of Re. If the body is sharp edged such as flat plate or disc held perpendicular to the flow, the point of separation is almost fixed and contribution of friction drag is negligibly small as compared to that of form drag. On the other hand for the case of flow past cylinder or sphere, the location of point of separation depends on the Reynolds number.

Out of these three types of drags i.e. deformation drag, form drag and friction drag, some can be measured and others can be computed. Since the relative contribution of these to the total drag depends on Reynolds number and body shape, problem of predicting the total drag on a body is not amenable to a complete analytical solution.

SAQ 2

(i) Define deformation drag.

(ii) Differentiate between form drag and friction drag.

(iii) Drag characteristics are greatly affected by Reynolds number and the body shape. Comment.

13.5 DRAG ON SPHERE

To understand the flow past sphere, it is desirable to know the analysis of steady flow of an ideal fluid around a sphere. Solution of the Laplace's equation with the necessary boundary condition will yield an expression for velocity distribution around sphere. Application of Bernoulli's equation will then yield pressure distribution. Since the flow pattern is symmetrical, the pressure distribution will also be symmetrical on the front and rear of the sphere as shown in Figure 13.5 (a). Since there is no viscosity, there is neither form drag nor friction drag indicating that there is no total drag. This inability of the theory of ideal fluid to yield results approximating those observed in experiments is known as D'Alembert's Paradox.

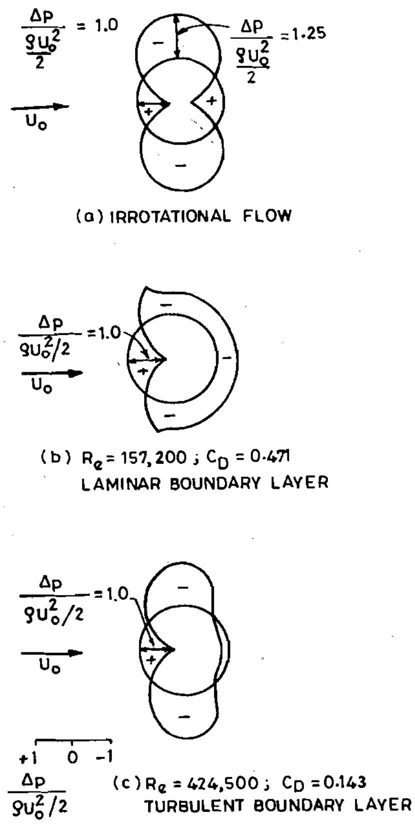

Figure 13.5 : Pressure Distribution around a Sphere

On the other hand when fluid possesses some viscosity, however small it may be, the flow pattern and the resulting pressure distribution are entirely different. If the Reynolds number defined as $\frac{U_0 D \rho}{\mu}$ is very small-say less than 0.2, the viscous forces are much more important than the inertial forces and therefore, Navier Stokes' equation can be integrated to yield the following expression,

$$F_D = 3\pi D \mu U_0 \tag{13.2}$$

or

$$C_D = \frac{\frac{F_D}{(\pi D^2/4)}}{\rho \frac{U_0^2}{2}} = \frac{24}{\text{Re}}, \tag{13.3}$$

wherein C_D is the coefficient of drag.

Equation (13.3) reveals that drag coefficient is inversely proportional to the Reynolds number. As mentioned earlier, for this case it can be proved that out of total drag $3\pi D \mu U_0$, the contribution due to form drag (i.e. deformation drag) is $\pi D \mu U_0$ and the contribution of the surface drag (friction drag) is $2\pi D \mu U_0$. Experimental observations show that upto a value of Re equal to 0.2, Stokes' law can be used to predict drag coefficient with a reasonable confidence provided the sphere is in motion in infinite fluid. Presence of the boundary of the container increases the resistance. For such a case, the drag coefficient can be computed by using the following equation :

$$C_D = \frac{24}{\text{Re}} \left[1 + 2.1 \frac{D}{D'} \right] \tag{13.4}$$

wherein D' is the diameter of container and D is the diameter of sphere.

Oseen (1927) pointed out that it is only in the vicinity of the sphere that the acceleration terms omitted by Stokes are very small compared to the viscous term. Far away from the sphere the case is exactly reverse. Therefore, he improved the Stokes analysis by including certain inertial terms and proposed the equation :

$$C_D = \frac{24}{\text{Re}} \left\{ 1 + \frac{3}{16} \text{Re} \right\} \qquad (13.5)$$

It can be observed from Figure 13.6 that Oseen's solution does not follow experimental trend and the upper limit of applicability of Oseen's solution is Re equal to 2.0.

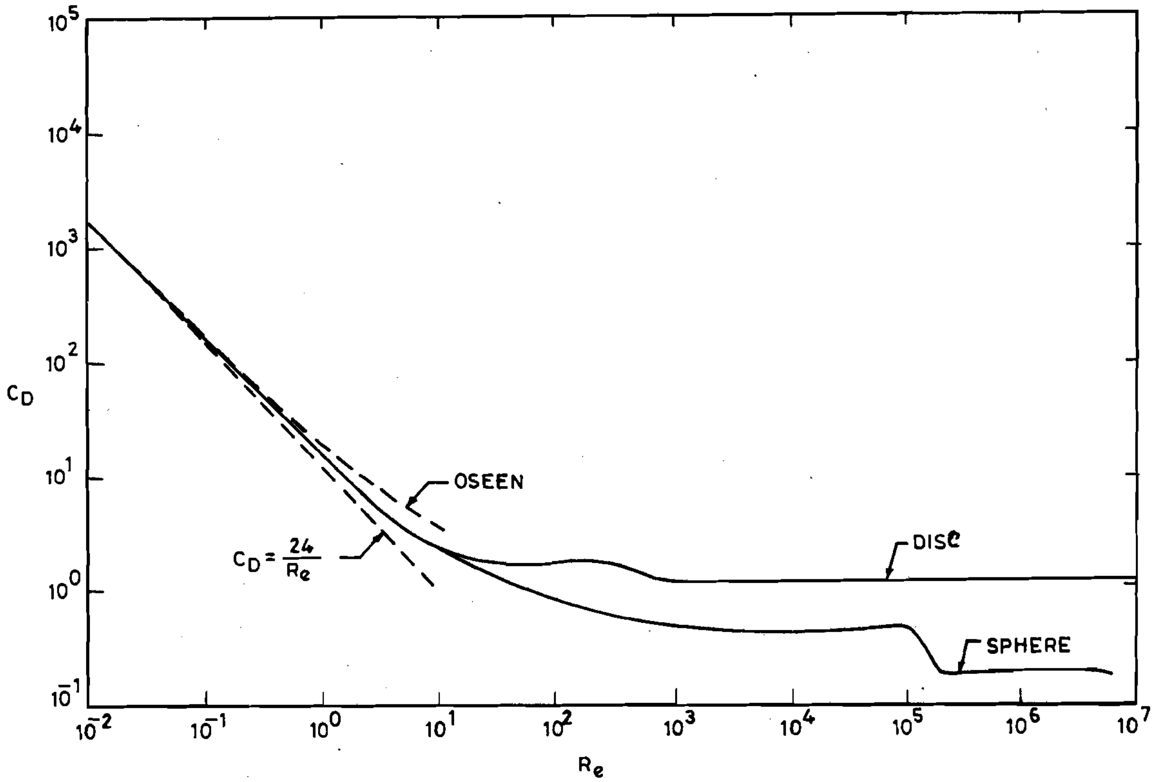

Figure 13.6 : Variation of C_D with Re

As the Re is further increased, the region in which the viscous deformation takes place is reduced considerably and is restricted to the laminar boundary layer. Furthermore, the boundary layer which is laminar increases in thickness and separates somewhat upstream of the point of maximum cross- section. The separation produces a wake behind the body which is laminar for low value of Re. The flow in the wake becomes unstable and continuous eddies are shed behind the body.

Figure 13.5 (b) shows typical pressure distribution around a sphere when boundary layer is laminar. It can be observed from this figure that the pressure distribution in the zone of accelerating flow is almost the same as that in the potential flow. Since the laminar boundary layer can stand only small adverse pressure gradients, the boundary layer separates at an angle of 80°. For Re between 0.50 and 10^4, the following empirical equation can be used

$$C_D = \frac{24}{\text{Re}} + \frac{3}{\sqrt{\text{Re}}} + 0.34 \qquad (13.6)$$

It can be observed from Figure 13.6 that C_D value changes from 0.4 to 0.5 over a range of Re from 10^3 to 10^5. This is so because in the this range of Re contribution of friction drag to the total drag is much small compared to that of form drag. This small increase in the value of C_D is due to the development of boundary layer and change in the character of the wake.

With further increase in the Reynolds number, the separating boundary layer can no longer remain laminar and it changes into turbulent boundary layer. Simultaneously at the same time, the point of separation shifts further downstream. The separation point is now located at 110 degrees approximately. Due to the change in point of separation, there is reduction in the size of the wake as well as in the value of C_D, which reduces from 0.5 to 0.2. Typical pressure distribution at such Re is as shown in Figure 13.5 (e). The Reynods number at which the separating boundary layer changes from laminar to turbulent is known as critical sphere. The actual value of this critical Reynolds number depends upon the roughness characteristics of the sphere and the level of turbulence present in the flow.

SAQ 3

(i) Define Stoke's law.

(ii) Sketch the variation of C_D with Re for a sphere.

(iii) At a certain value of Re, there is a sudden drop in the value of C_D in case of a sphere. What is this value of Re? Also explain the reason for such a drop in C_D.

13.6 DRAG ON CYLINDER

Analytical solution for the drag experienced by an infinite cylinder placed in uniform stream has been put forward by Lamb. His analytical solution is valid upto a value of Reynolds number equal to 0.2. It has been observed that experimental points start deviating from the results obtained on the basis of theoretical analysis at Reynolds number greater than 0.20. Drag coefficient for cylinder also decreases with increase in Reynolds number in a manner similar to the case of sphere. Oseen's approximate method can also be extended for drag experienced by cylinder for low values of Reynolds number (say Re = 2 or 3). With increase in Reynolds number, the flow pattern becomes asymmetrical about the axis perpendicular to the direction of flow. It has been observed that at Re equal to 4.0, very weak vortices are formed behind the cylinder. This is shown in Figure 13.7 (b). Alongwith these vortices, wake is also formed and flow keeps on recirculating in this region. If the Reynolds number is further increased upto a value of 20, the wake behind the cylinder becomes more predominant and so also the vortex pair as shown in Figure 13.7 (c). If the Reynolds number is again increased, these vortices get stretched and become unsymmetrical and they leave the cylinder with relatively smaller velocity. The various flow patterns around a cylinder for various Reynolds number are shown in Figure 13.7.

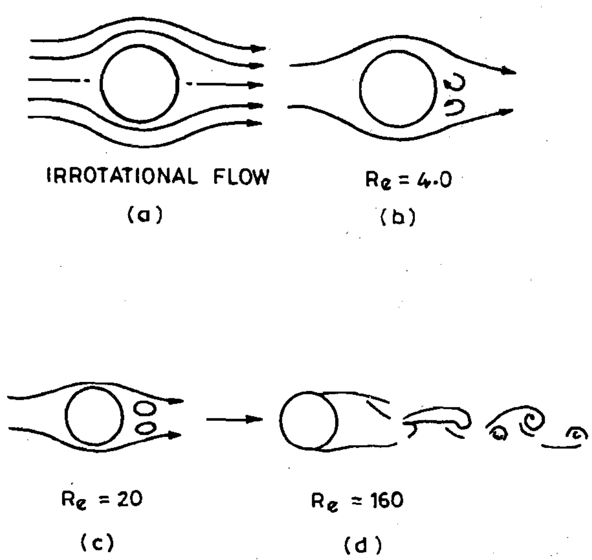

Figure 13.7 : Flow around an Infinite Cylinder

13.6.1 Karman Vortex Trail

As mentioned above when Reynolds number is increased beyond 30, the two vortices behind the cylinder get stretched and become unstable. As a consequence of this, they are transported down and another two vortices are created in place of these transported vortices. This process continues. Under such circumstances, the wake behind the cylinder consists of a series of vortex pairs moving in the downstream direction with relatively smaller velocity.

Karman was the first who gave explaination of this phenomenon and hence this is widely known as **Karman Vortex Trail**. According to him, there are two possible combinations of these vortex pairs as shown in Figures 13.8 (a) and 13.8 (b). Analysis of stability of these vortices revealed that configuration (a) is unstable and configuration (b) is also unstable except when $\frac{a}{b} = \cosh^{-1}\sqrt{2} = 0.281$.

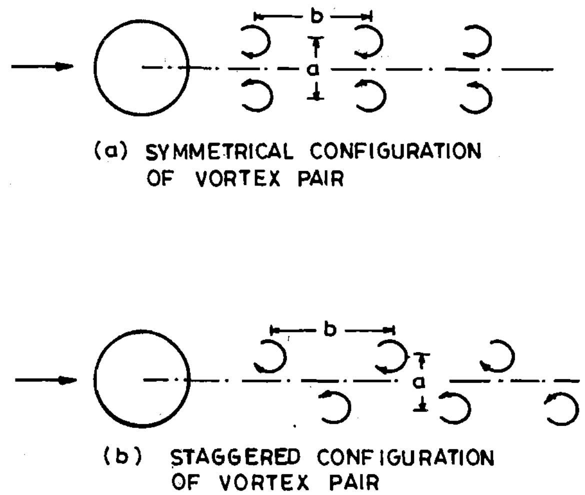

Figure 13.8 : Karman Vortex Trail

Taylor has given the following relationship for the frequency with which these vortices are shed from one side of the cylinder

$$f = 0.198\frac{U_o}{D}\left\{1 - \frac{19.7}{\text{Re}}\right\} \tag{13.7}$$

wherein U_0 is the velocity of flow and D is the diameter of the cylinder. The dimensionless quantity $f\frac{D}{U_o}$ is commonly known as **Strouhl number**. It has been found that over the range of Re from 120 to 20,000, equation (13.7) gives $f\frac{D}{U_o} = 0.17$ to 0.20. Recent experimental observations have revealed that upto Re equal to 10^5, the value of $f\frac{D}{U_o}$ for cylinder is equal to 0.20.

Due to alternate shedding of the vortices, a periodic force is experienced by the cylinder in the direction perpendicular to the flow. If the frequency of this lateral force is equal to the natural frequency of the cylinder, resonance will take place and lateral forces of large magnitudes will be generated. Such considerations are much more important in aerodynamic study of suspension bridges. Figure 13.9 shows the variation of Strouhl number, S, with drag coefficient C_D.

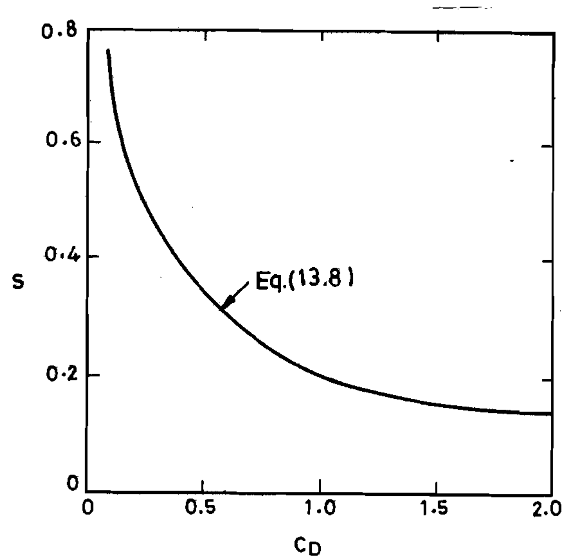

Figure 13.9 : Variation of S with C_D for a Cylinder

The variation shown in Figure 13.9 could be expressed by the equation :

$$S = \frac{0.21}{C_D^{0.75}} \tag{13.8}$$

SAQ 4

(i) Giving sketches, explain Karman vortex trail.

(ii) Define Strouhl number and give its significance.

13.7 DRAG ON FLAT PLATE

Flow pattern of irrotational flow for the case of flow past a plate held perpendicular to the direction of flow is depicted in Figure 13.10 (a). Since the flow considered is irrotational, stream line pattern is symmetrical on both sides of the plate.

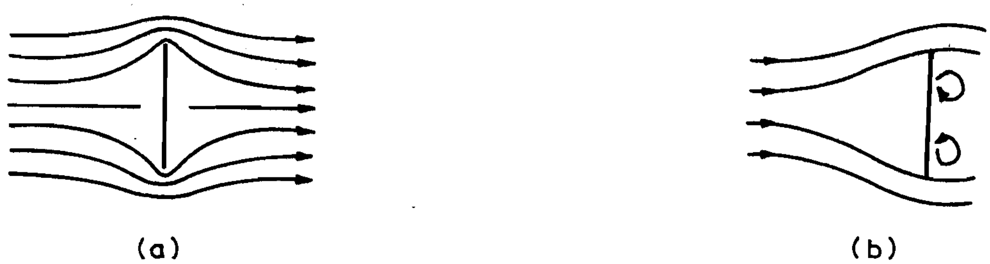

Figure 13.10 : Flow Pattern around a Flat Plate

For such a case no separation takes place and due to the symmetrical flow pattern, the pressure distribution will also be symmetrical and hence no pressure drag will be experienced by the plate. But on the other hand, if flow of real fluid is considered, the flow pattern will be totally different as shown in Figure 13.10 (b). The flow will separate at both the ends of the plate and because of this, the pressure behind the plate will be smaller as compared to that on the front side. For such a case C_D is a function of Reynolds number for low and moderate values of Re. It has been observed that once Re exceeds about 10^3, C_D attains a constant values of about 1.9 if the plate is infinitely long. Flow will not be truely two dimensional if the plate is not sufficiently long and hence the drag coefficient will be smaller. Variation of C_D with B/L for high values of Re is shown in Figure 13.11.

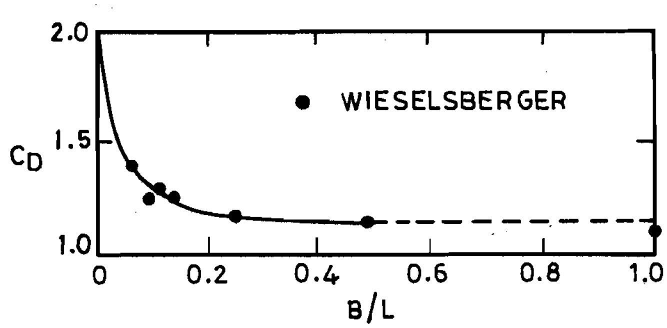

Figure 13.11 : Variation of C_D with B/L for a Rectangular Plate held Perpendicular to the Flow

For the case of disc, C_D varies with Re in a similar manner as that for a plate held perpendicular to the flow. But due to the three dimensional character of the flow, the limiting value of drag coefficient is 1.10 which is smaller than the drag coefficient for flat plate (see Figure 13.6).

13.8 DRAG ON AN AIRFOIL

Consider a case of flow around an airfoil as shown in Figure 13.12. Airfoil body is a well stream line body and hence flow can only separate at the rear end of the airfoil.

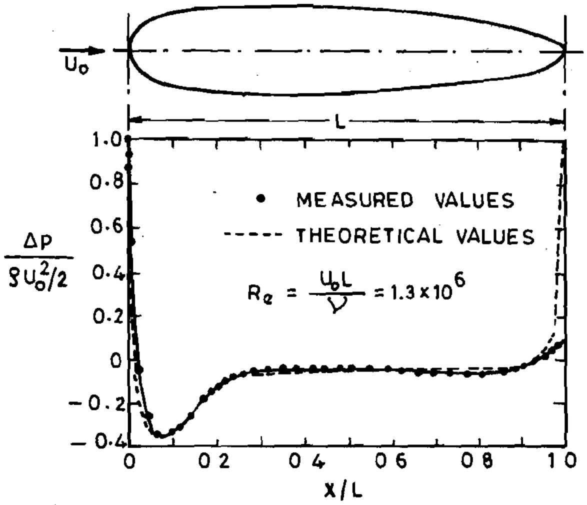

Figure 13.12 : Pressure Distribution around an Airfoil

On account of the nature of streamlining that airfoil body has at relatively high values of Reynolds number, the major contribution to the total drag is even of the friction drag and contribution of form drag (pressure drag) is comparatively very small. Measured pressure distribution and the predicted pressure distribution using theory of irrotational flow are shown in Figure 13.12. Close observation of this figure reveals that both the pressure distributions agree very well except at the rear end. It has been observed that for the case of airfoil, drag coefficient mainly depends on Reynolds number and shape, but a sudden drop in the value of C_D as in the case of sphere or cylinder is not found. The main reason for this is that change from laminar to turbulent boundary layer does not alter the wake size significantly to affect the contribution of form drag.

Table 13.1 gives C_D values for several geometrical shapes of bodies and Table 13.2 gives a list of drag coefficients of practical body shapes.

TABLE 13.1 : Drag Coefficient for Various Body Shapes

Body Profile	Reynolds Number Re	Drag Coefficient C_D
Circular Cylinder (Infinite)	10^4 to 2×10^5	1.20
Circular Cylinder (Infinite)	5×10^5	0.35
Elliptical Cylinders		
2 : 1	5×10^4	0.46
	10^5	0.60
4 : 1	2.5×10^4 to 10^5	0.32
8 : 1	2.5×10^4	0.29
	2×10^5	0.20
Triangular Cylinders 120°	→▶ 10^4	2.00
120°	→◀ 10^4	1.72
60°	→▶ 10^4	2.20
60°	→◀ 10^4	1.39
30°	→▶ 10^4	1.80
30°	→◀ 10^5	1.00
Hemispheres (hollow)	→◗ 10^4	1.33
	→◖ 10^3 to 10^5	0.34
	→⊃ 4×10^4	2.30
Semitubular Cylinders	→⊂ 4×10^4	1.12
	→◗ 3.5×10^4	2.00
Square Cylinders	→◆ $10^4 \times 10^5$	1.60

TABLE 13.2 : Drag Coefficient of Some Practical Bodies

	Body Profile	Drag Coefficient
1.	Empire State Building, New York, about 380 m high	1.30 to 1.5 (depending on wind direction)
2.	"Trylon" slender pyramidal building 206 m high with 20 m wide base	0.80 to 1.43 (depending on wind direction)
3.	Wind resistance of several ships	0.20 to 0.70
4.	A man falling down vertically	1.0 to 1.30
5.	Volkswagen passenger car	0.50
6.	Minibus	0.73
7.	Non Streamlined engine with five bogies	1.90

13.9 ILLUSTRATIVE EXAMPLES

Example 13.1 :

Alluminium ball of diameter 2.0 mm having relative density 2.80 is falling freely in a tank containing fluid which has mass density of 910.2 kg/m^3. If the velocity of ball is 0.35 cm/s, determine the dynamic viscosity of oil.

Solution :

Initially let us assume flow to be within Stoke's range.

According to Stokes' law, drag force is given by

$$F_D = 3\pi \mu D U$$

Submerged weight of the ball is given by

$$= \pi D^3 \frac{(\gamma_s - \gamma)}{6}$$

wherein γ_s and γ are the specific weights of the solid and fluid respectively.

Equating the two forces one gets

$$\mu = \frac{D^2}{18\,U}\left(\gamma_s - \gamma\right)$$

$$= \frac{2.0^2 \times 10^{-6}}{18 \times 0.35 \times 10^{-2}} \,(2.8 \times 1000 - 910.2) \times 9.81$$

$$\therefore \quad \mu = 1.177 \text{ kg/ms}$$

Now it should be checked whether for this viscosity, Reynolds number is within Stokes' range

$$\text{Re} = \frac{U D \rho}{\mu}$$

$$= \frac{0.35 \times 10^{-2} \times 2 \times 10^{-3} \times 910.2}{1.177}$$

$$= 0.541 \times 10^{-2}$$

Since Re is less than 0.2, assumption is justified.

Example 13.2 :

A sphere of diameter 2.5 cm having relative density of 2.65 is freely falling in a tank of oil having mass density 898 kg/m^3 and kinematic viscosity of 1.58 x 10^{-4} m^2/s. Compute the fall velocity of the sphere and the drag force.

Solution :

Drag Force

$$F_D = C_D \frac{\rho U^2}{2} \frac{\pi D^2}{4}$$

Also,

$$F_D = \frac{\pi D^3}{6} \left(\gamma_s - \gamma\right)$$

Thus, the drag force can be calculated straight way as

$$= \frac{3.142 \times 2.5^3 \times 10^{-6}}{6} \left(2.65 \times 1000 - 898\right) \times 9.81$$

$$= 0.1406 \text{ N}$$

However a trial and error method is required to compute fall velocity because it needs C_D which itself depends on fall velocity.

Steps are as follows,

(i) Assume Re

(ii) Compute C_D by using equation (13.6) which is

$$C_D = \frac{24}{\text{Re}} + \frac{3}{\sqrt{\text{Re}}} + 0.34$$

(iii) Use this value of C_D in drag equation to calculate U.

(iv) Compute the value of Re using the value of U as obtained in step (iii)

(v) If Re computed in step (iv) is same as in step (i) o.k., otherwise assume a new value of Re and repeat the steps.

Assume Re = 100

$$C_D = \frac{24}{100} + \frac{3}{\sqrt{100}} + 0.34 = 0.88$$

$$U = \frac{8 F_D}{C_D \rho \pi D^2}$$

$$= \frac{8 \times 0.1406}{0.88 \times 898 \times 3.14 \times 2.5^2 \times 10^{-4}}$$

$$= 0.725 \text{ m/s}$$

and

$$\text{Re} = \frac{0.725 \times 2.5 \times 10^{-2}}{1.58 \times 10^{-4}}$$

$$= 115$$

Assume Re = 115

This gives $C_D = 0.828$

$U = 0.77$ m/s

and Re = 122 o.k.

Hence fall velocity of the sphere is 0.77 m/s.

Example 13.3 :

A truck having a projected area of 6.5 m^2 travelling at 80 km/hr experiences a total resistance of 2 kN. Out of this, the form drag is 60%. Calculate the coefficient of form drag. Assume specific weight of air as 12 N/m^3.

Solution :

Total resistance = 2×10^3 N.

Form drag = $0.6 \times 2 \times 10^3 = 1.2 \times 10^3$ N

For form drag, one can write

$$F_D = C_D \frac{\rho U^2}{2} \times \text{Projected Area}$$

(Here U is the velocity of truck.)

$$\therefore \quad C_D = \frac{2 F_D}{\rho U^2 \times \text{Projected Area}}$$

$$\text{As} \quad U = \frac{80 \times 1000}{3600} = 22.22 \text{ m/s}$$

One gets $C_D = 0.61$.

Example 13.4 :

Electric transmission towers, 10 m high, are fixed 400 m apart to support 10 cables, each of 20 mm diameter. Determine the moment acting at the base of each tower when a wind flows with a velocity of 100 km/hr. Assume mass density of air as 1.2 kg/m^3 and μ (air) as 1.6×10^{-5} kg/ms. Also calculate the frequency of vortex shedding.

Solution :

For drag force

$$F_D = C_D \frac{\rho U_0^2}{2} A$$

and

$$\text{Re} = \frac{U_0 D \rho}{\mu}$$

Here

$$U_0 = \frac{100 \times 1000}{3600} = 27.77 \text{ m/s}$$

$$\text{Re} = \frac{27.77 \times 1.2 \times 0.02}{1.6 \times 10^{-5}} = 4.16 \times 10^4$$

Projected Area $A = 400 \times 0.02 = 8 \text{ m}^2$

Using equation (13.6)

$$C_D = \frac{24}{\text{Re}} + \frac{3}{\sqrt{\text{Re}}} + 0.34$$

$$= \frac{24}{4.16 \times 10^4} + \frac{3}{\sqrt{4.16 \times 10^4}} + 0.34$$

$$= 0.355$$

Therefore, drag force on each wire of 400 m long

$$= 0.355 \times 1.2 \times \frac{27.77^2}{2} \times 8$$

$$= 1315.83 \text{ N}$$

Moment at the base = $1315.83 \times \frac{10}{2} = 6579.15$ Nm

Using equation (13.7) for the frequency of vortex shedding

$$f = 0.198 \frac{U_0}{D} \left(1 - \frac{19.7}{\text{Re}}\right)$$

$$= 0.198 \times \frac{27.77}{0.02} \left(1 - \frac{19.7}{4.16 \times 10^4}\right)$$

$$= 274.87 \text{ Hz}$$

13.10 SUMMARY

In this unit the forces exerted on bodies exposed to flow of fluid have been discussed. The importance of flow separation in affecting these forces has also been emphasised. The methods for avoiding or controlling the separation were discussed. It was seen that the laminar boundary layer is more susceptible to separation than the turblent boundary layer.

Commonly encountered body shapes such as sphere, cylinder, flat plate and airfoil were considered while studying their drag characteristics. Relationships were studied for the variation of C_D with Re for different body shapes. Attention was also drawn to the vortices and their characteristics that one has in the wake region of these bodies.

13.11 KEY WORDS

Drag : Force exerted by fluid on the body in the direction of fluid flow.

Separation : Flow conditions in which velocities near the wall are negative, cause flow to separate from the wall, promoting instability, eddy formation and large energy dissipation. This phenomenon is called separation.

Boundary Layer : Fluid layer of retarded flow that is formed next to the boundary is known as boundary layer. In this layer marked velocity changes take place.

Surface Drag : Force due to friction of the fluid against the body is known as surface drag.

Pressure Drag : Pressure drag or form drag is due to separation of the boundary layer and the resulting pressure difference between the front and the wake region of the boundary.

Drag Coefficient : Drag force per unit area divided by the dynamic head is known as drag coefficient and is designated by C_D.

Strouhl Number : It is a dimensionless number used for studying the vortex shedding from an immersed body.

Pressure Distribution : Variation in pressure around the body is known as pressure distribution. It could as well define variation in pressure in a particular region of flow, for example, in the wake behind the body.

13.12 ANSWERS TO SAQs

Check your answers of all SAQs with respective preceeding text of each SAQ.